Microchimica Acta (2020) 187:396
https://doi.org/10.1007/s00604-020-04381-w

ORIGINAL PAPER

A fiber optic nanoplasmonic biosensor for the sensitive detection of ampicillin and its analogs

Pallavi P. Chaudhari[1] · Lai-Kwan Chau[1,2] · Yen-Ta Tseng[1] · Chun-Jen Huang[3] · Yuh-Ling Chen[4]

Received: 6 February 2020 / Accepted: 9 June 2020

Abstract

A novel optical immunosensor for the screening of ampicillin (Amp) residues has been developed. The biosensor is based on fiber optic particle plasmon resonance detection and uses an enhancement method called as fiber optic nanogold-linked immunosorbent assay (FONLISA) for the sensitive detection of antibiotics. A commercial antibody which had a higher affinity for ampicillin than for other β-lactam antibiotics was chosen. A surface competitive binding assay was used in which a fixed concentration of antibiotic-conjugated gold nanoparticles (AuNPs) competes with free unlabeled antibiotic molecules to measure the amount of binding with antibody molecules immobilized on an optical fiber. The synthesis of the 11-mercaptoundecanoic acid (MUA)-ampicillin conjugate facilitates the attachment of the Amp molecules to AuNPs via MUA which acts as a linker between them. This AuNP–Amp conjugate was then used for the detection of β-lactam antibiotics. The practical limit of detection obtained for Amp was 0.74 ppb (7.4×10^{-10} g/mL) which is lower than the recommended maximum residue limit (MRL) for β-lactams. The method also shows a wide linear range of 4 orders. Its applicability to the determination of ampicillin in spiked milk samples has been demonstrated with good recovery and reproducibility.

Keywords Biosensor · Fiber optic · Immunoassay · Nanoplasmonic · Gold nanoparticle · Antibiotics · β-Lactam

Introduction

An increase in the human population has driven up the demand for livestock consumption. Globally, the products of animal origin consumption contribute 17% to kilocalorie consumption and 33% to protein consumption [1]. Due to the increased demands of livestock production, the consumption of antibiotics by the animal and poultry industries has also increased. Antibiotics are used in animal rearing to prevent diseases and for therapeutic purposes. The most commonly used antibiotics are β-lactams. Some β-lactams have also been reported to be used as feed additives which act as growth enhancers for poultry and swine [2–4]. The overuse of antibiotics has resulted in the development of drug-resistant bacteria which pose a serious risk to animal and human health [5–9]. As a measure of precaution, the European Union has banned all nontherapeutic antimicrobials (NTAs). The maximum residue limit (MRL) for β-lactam antibiotics has been set to be 4 μg/kg in milk and 50 μg/kg in animal tissues (EU Regulation no 37/2010). Similarly, very strict regulations have been set up by other countries about the MRLs of β-lactam antibiotics in animal products. So it becomes necessary to develop a sensitive and fast sensor to detect the β-lactam antibiotics in animal products.

A number of methods have been reported for the detection of β-lactam antibiotics in different matrices such as water and animal products. In general, these methods can be classified into two groups: confirmatory and screening [10]. Confirmatory methods are mostly based on liquid chromatography (LC) coupled to mass spectrometry (MS) to quantify

Electronic supplementary material The online version of this article (https://doi.org/10.1007/s00604-020-04381-w) contains supplementary material, which is available to authorized users.

✉ Lai-Kwan Chau
chelkc@ccu.edu.tw

[1] Department of Chemistry and Biochemistry, National Chung Cheng University, Chiayi 62102, Taiwan

[2] Center for Nano Bio-Detection, National Chung Cheng University, Chiayi 62102, Taiwan

[3] Department of Biomedical Sciences & Engineering, National Central University, Jhong-Li, Taoyuan 320, Taiwan

[4] Institute of Oral Medicine, National Cheng Kung University, Tainan 70101, Taiwan

Published online: 20 June 2020

analyte concentration [11–13]. However, such methods are time-consuming, expensive, and require sophisticated equipment and trained personnel. Screening methods can detect an analyte or a family with ideal characteristics such as high throughput, ease of use, short analysis time, and low cost. Several commercial microbial inhibition tests are available for screening of β-lactam antibiotics [14, 15]. However, this approach exhibits limited specificity and sometimes gives false positives due to natural inhibitors. Interpretation of results is subjective and may lead to false negatives and positives. In addition, it requires constant monitoring of the strains to ensure they have not become resistant to antibacterials.

Immunological methods are more specific and have been classified according to the detection label: enzyme-linked immunosorbent assays [16] and fluoroimmunoassay [17]. Nevertheless, the need for a rapid and low-cost test with a low limit of detection (LOD) has encouraged the development of biosensors for the detection of β-lactam antibiotics. The bioreceptors in these biosensors can be based on enzyme inhibition [18], immunological [19–21], bacterial receptor proteins [22], DNA aptamers [23], and molecular imprinting [24]. Among the transducers used in biosensors for antibiotic residues, optical detection is the most used format [25]. However, the detection of small molecules with low LOD still remains a challenge using the optical sensors.

Herein, an assay was developed for the detection of ampicillin (Amp) and its analogs using a fiber optic particle plasmon resonance (FOPPR) biosensing system [26–28] based on a direct competition assay using ampicillin-conjugated gold nanoparticles (AuNP@Amp). As an antibody-based optical sensor is the most often used biosensor for antibiotic residues, we chose β-lactam antibiotic ampicillin as a model to design an antibody-based FOPPR biosensor for ampicillin and its analogs. The FOPPR biosensor is based on nanoplasmonic absorption by gold nanoparticles (AuNPs) via fiber-optic evanescent wave excitation. When light propagates in an optical fiber via multiple total internal reflections (TIR), the evanescent wave on the fiber core surface excites the particle plasmon resonance (PPR) of AuNPs on the surface and thus, the light transmitted through the fiber is attenuated by interaction with the AuNPs. The multiple TIRs increase the optical path length and the excitation of guided modes in TIR drastically increases light/matter interaction [29, 30], thus resulting in large sensitivity enhancement in biosensing measurements. Since the FOPPR sensing system is a versatile platform, it can easily be converted to biosensors based on receptors or aptamers.

Recently, a new enhancement method called fiber optic nanogold-linked immunosorbent assay (FONLISA) was used to improve the sensitivity of the FOPPR biosensor [28]. The instrumentation used in this method is identical to that of the traditional label-free direct assay in FOPPR biosensor. The difference lies in the design of the biosensor which greatly affects the sensitivity of the sensor. In the traditional method (Fig. 1a), the signal is obtained by calculating the change in intensity caused by the specific binding of the recognition molecule with the analyte present on the surface. Since the surface is already coated with AuNPs, this change is proportional to the change of absorption coefficient ($\Delta\alpha$) of the AuNP layer. In the FONLISA method (Fig. 1b), no AuNPs are present on the fiber surface at the beginning so the change in intensity is calculated from the absolute increase of absorption coefficient (α) against the zero absorbance background. As α typically is several orders of magnitude larger than $\Delta\alpha$ [31], the FONLISA method leads to higher signal, higher sensitivity, and lower limit of detection.

Experimental

Reagents and materials

Ampicillin sodium salt was purchased from Biovision (USA). Penicillin G sodium salt was purchased from Acros Organics. Levofloxacin was purchased from Tokyo Chemical Industries. Amoxicillin, nitrofurantoin, and aminoundecyltriethoxysilane (AUTES) were purchased from Alfa Aesar. Hydrogen tetrachloroaurate trihydrate ($HAuCl_4$) was purchased from Showa Chemical Industry. Mercaptoundecanoic acid (MUA), 6-mercapto-1-hexanol (MCH), (3-mercaptopropyl)-trimethoxysilane (MPTMS, 98%), and bovine serum albumin (BSA) were purchased from Sigma Aldrich while disuccinimidyl suberate (DSS) was purchased from Ark Pharm, Inc. 4-Dimethylaminopyridine (DMAP) and N,N′-dicyclohexylcarbodiimide (DCC) were obtained from BCH pharmaceuticals. Dichloromethane (DCM) was purchased from Emsure. Ethanolamine was purchased from Janssen Chimica. Tris(hydroxymethyl)aminomethane (Tris) was purchased from J.T.Baker. Sulfuric acid was purchased from Applichem. Sodium chloride (NaCl) was obtained from Honeywell. Sheep polyclonal anti-penicillin antibody (ab30592), mouse immunoglobulin G (IgG) (ab198772), and horseradish peroxidase-conjugated goat anti-mouse IgG (anti-IgG-HRP, ab6789) were obtained from Abcam. ELISA plate (Nunc MaxiSorp™, 44-2404-21) was purchased from ThermoFisher Scientific. 3,3′ 5,5′-Tetramethylbenzidine (TMB) substrate kit was purchased from ThermoFisher Scientific.

Sulfobetaine silane (SBSi) was synthesized according to previously reported work [32]. All the aqueous solutions were made with purified water through a Millipore system (18.2 MΩ cm, Millipore). The phosphate-buffered saline (pH 7.4) used in this study was obtained from Diasorin Inc. (USA). Full fat milk was obtained from a local grocery store. The microfluidic chips were manufactured by an injection molding technique using polycarbonate. The design and fabrication procedures have been described previously [33].

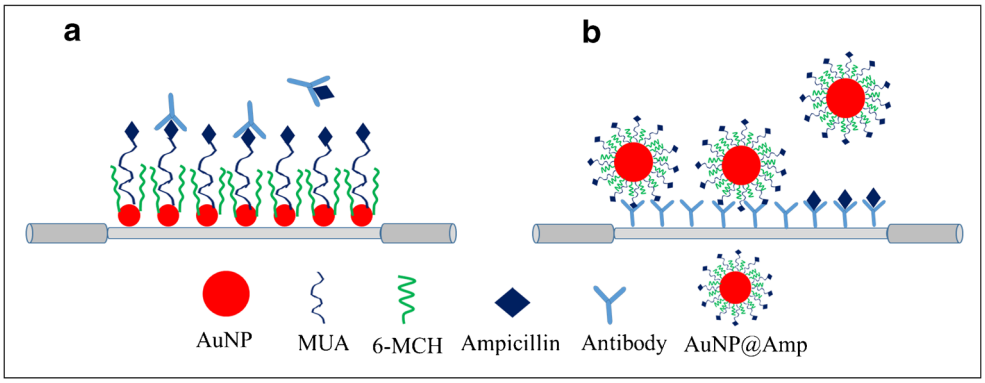

Fig. 1 (a) Graphical abstract of the traditional assay. (b) Graphical abstract of the FONLISA

Synthesis of AuNPs

AuNPs were synthesized according to the previously reported procedure [34]. A 20 mL solution of 0.88 mM $HAuCl_4$ was heated until vigorous boiling was observed with bubbling and was stirred continuously throughout the synthesis. Then, 2.4 mL of 1% sodium citrate solution was added in the boiling solution all at once. It was observed that the color of the solution transitioned from golden yellow to completely colorless to dark purple and finally converting to a ruby red color. This solution was boiled for 20 min, then cooled down to room temperature with stirring continued during the cooling down process.

Preparation of MUA–Amp conjugate

A solution of 1 mmol of MUA and 0.2 mmol DMAP in 10 mL DCM was stirred and allowed to react for 2 h. This solution was then added dropwise to a mixture of 1 mmol of ampicillin sodium salt and 1.2 mmol DCC in DCM at 0 °C. The resulting mixture was then stirred for 48 h at room temperature and then filtered and dried using a rotary evaporator and high vacuum [35]. A yellow colored solid was obtained which was further used without any purification (Scheme 1). Attaching the terminal alkyl thiol group to ampicillin facilitates its adsorption on the AuNP surface.

Preparation of AuNP@Amp conjugate

The AuNP@Amp conjugate can be visualized as shown in Fig. 2. In order to form a mixed self-assembled monolayer (SAM) on the AuNP surface, an AuNP solution was mixed with an equal volume of Tween-20 (2 mg/mL) and allowed to stand for 30 min. Tween-20 is a nonionic surfactant that stabilizes the AuNPs [36]. These Tween-20 capped AuNPs were then used for the preparation of the AuNP@Amp conjugate. In order to obtain a well-ordered SAM on AuNP surface, 400 μL of a mixed solution containing the MUA–Amp crude compound (0.7 mg/mL) and 6-MCH (1.2 mM) in methanol with the volume ratio of 1:5 was added to 1.6 mL of the AuNP solution. The ratio of MUA–Amp and MCH (1:5) has not been optimized yet but preliminary results show that the sensitivity of the biosensing system is not significantly affected by the ratio. In addition, various concentrations of MUA–Amp in increments of 0.05 mg/mL were added to the AuNP solution to test the saturation point, adding 0.75 mg/mL causes aggregation of the AuNPs in solution and turns it purple. The resulting solution was incubated for 18 h to allow the alkane thiols to be well adsorbed on the surface of AuNPs [37, 38]. The solution was then centrifuged at 10,000 rpm for 20 min, the supernatant was removed, and the centrifugate was dissolved in PBS and centrifuged again at same conditions. The concentration of the AuNP@Amp solution was maintained by adding a PBS solution to the centrifugate.

Preparation of sensor fibers

The optical fibers were cleaned with a soap solution and rinsed with water followed by ethanol and then thoroughly cleaned with ultrapure water and dried using nitrogen. The fibers were then cleaned with Piranha solution (mixture of 30% H_2O_2 and H_2SO_4 1:3 v/v) and subsequently annealed in an oven at 110 °C overnight. After the fibers were cooled down, they were treated with oxygen plasma to remove any residual surface contaminants. The fibers were then immersed in a solution consisting of 10 mM SBSi and 5 mM AUTES in anhydrous ethanol for 18 h. After washing with ethanol and then rinsing with ultrapure water, the fibers were immersed in a 0.08 M solution of DSS in DMSO overnight. Finally, the fibers were washed first with DMSO and then with PBS to remove any excess unbound compounds. These surface-activated fibers were then used to immobilize the anti-penicillin antibody on the fiber core surface by immersing them in 0.1 mg/mL of the antibody solution for 4 h. The biofunctionalized fibers were then treated with 1 M ethanolamine (pH 8.5) for 30 min to remove the unbound antibody molecules and to deactivate any unreacted sites and then rinsed with PBS solution for further experiment.

Scheme 1 Proposed reaction for the synthesis of MUA–Amp

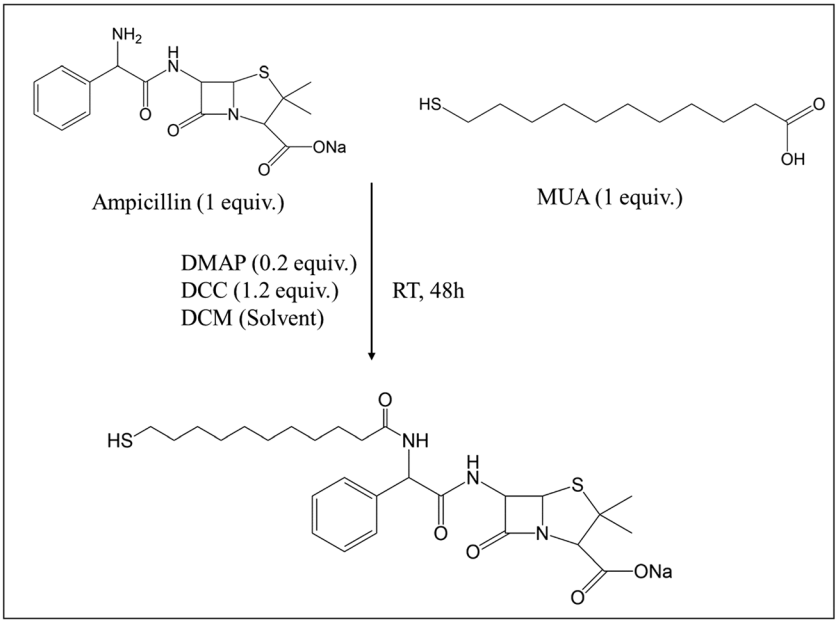

Quantitation of immobilized antibody on fiber surface by ELISA

The amount of mouse IgG that can be immobilized on the SBSi/AUTES-modified fiber surface was quantified using anti-IgG-HRP. A standard calibration curve was obtained by preparing a series of solutions (0.5 to 15 ng) of mouse IgG in PBS which were then incubated in wells of an ELISA plate for 18 h. The solution was aspirated from the wells, washed thrice with TBST (20.0 mM Tris, 150 mM NaCl, 0.1% Tween-20, pH 7.4) solution, and then the unbound sites on the plate were blocked with BSA (1.0 mg/mL) for 30 min. Afterwards, the contents were aspirated and the wells were washed with TBST solution. Then, a solution of anti-IgG-HRP (60 μL, 0.04 μg/mL) was injected in each well. After 60 min, all solutions were removed and the plate was washed with TBST buffer. Sixty microliters of TMB substrate was added to each well and incubated for 15 min. The reaction was stopped with 60 μL 2 M sulfuric acid. The absorbance of each well was measured at 450 nm. To measure the amount of mouse IgG immobilized on the fiber surface, the optical fibers were modified and activated using AUTES, SBSi, and DSS as previously described. Mouse IgG (0.1 mg/mL) was then immobilized on the fiber surface. The biofunctionalized fibers were then treated with BSA (1 mg/mL) for 15 min to minimize nonspecific adsorption and then rinsed with TBST solution. Then, the fibers were immersed in a solution of anti-IgG-HRP (60 μL, 0.04 μg/mL). After 60 min, the solution was removed and the fibers were washed with TBST buffer. Subsequently, the fibers were immersed in a 60 μL TMB substrate for 15 min. The reaction was stopped with 2 M sulfuric acid. The absorbance of each solution was measured at 450 nm. The results were performed in triplicate and the standard deviation was calculated in each case.

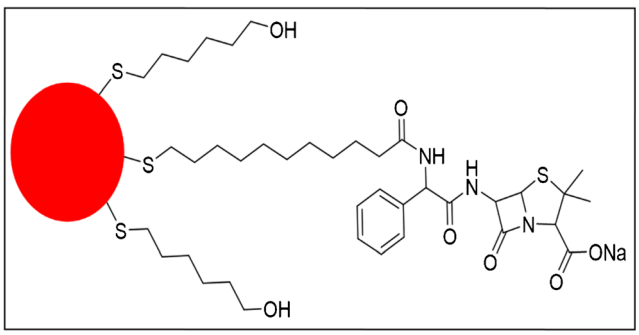

Fig. 2 Schematic representation of the mixed self-assembled monolayer formed on the surface of an AuNP

Biosensing system

Our biosensor system as shown in Fig. 3 consists of a light-emitting diode (LED, model IF-E93, Industrial Fiber Optic, Inc.) with a peak wavelength of 530 nm, a LED driver circuit to drive the LED with 1-kHz frequency modulation (home-made), a FOPPR sensor chip that holds the biofunctionalized fiber as described in the "Preparation of MUA–Amp conjugate" section, a photodiode (S1336-18BK, Hamamatsu), a photoreceiver amplification circuit (home-made), a power supply (PMT-D1V100W1AA, Delta Electronics), a signal acquisition module (NI-9234, National Instruments), and a graphical user interface programmed by LabVIEW® (National Instruments).

Quantitative analysis is performed by comparing the normalized transmitted light intensity of the sensor in a blank (I_M/I_0) to that in a sample containing an analyte (I_S/I_0), where I_0, I_M, and I_S are the steady-state transmitted light intensities of the sensor in a buffer solution, a blank containing a fixed concentration of AuNP@Amp conjugates in the absence of the analyte, and a

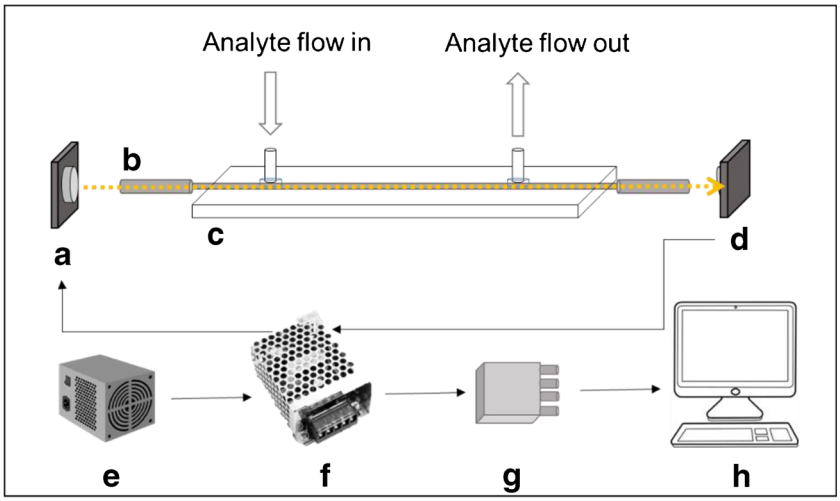

Fig. 3 Schematic representation of the experimental setup used for the FOPPR biosensor. The setup consists of a, light-emitting diode; b, sensor fiber; c, sensor chip; d, photodiode; e, power supply; f, LED driver and photoreceiver amplification circuits; g, data acquisition card; h, computer. The line arrows indicate the direction of flow of electricity and the dotted yellow arrow represents the direction of flow of light

sample containing a fixed concentration of AuNP@Amp conjugates in the presence of the analyte, respectively. A calibration curve is set up by plotting the sensor response, $(I_S - I_M)/I_0$, which is the difference in the normalized transmitted light intensity of the sensor in the sample to that in the blank, versus log concentration of the analyte. The use of normalized intensity provides a means to allow a certain variation of I_0 and thus alleviates the demand for precise optical alignment [39].

Nonspecific adsorption tests

In order to test the nonspecific adsorption of modified AuNPs onto the sensor fiber, three different approaches were used. For the first approach, the AuNPs were coated only with a monolayer of 6-MCH (1.2 mM in MeOH), to form AuNP@MCH. This solution was then injected in a sensor chip consisting of the antibody-functionalized sensor fiber as described earlier.

For the second approach, the AuNPs were conjugated with BSA (10^{-5} g/mL) (AuNP@BSA) using the following procedure. The AuNPs were mixed with an equal volume of Tween-20. A mixture of MUA (0.5 mM) and MCH (0.5 mM) in the ratio of 1:4 (v/v) was then added to the AuNP solution and allowed to incubate overnight. The mixture was then centrifuged, the supernatant was removed, and the centrifugate was rediluted to the original volume to maintain the concentration. Fifty microliters of EDC (2 mg/mL) and NHS (2 mg/mL) solution in PBS buffer was then added to the AuNP solution. This solution was then centrifuged, the supernatant was removed, and the centrifugate was diluted to the original volume. Then, 100 μg/mL of BSA was added to the solution and allowed to incubate for 1 h. The centrifugation process was repeated and then, the solution was injected in the sensor chip.

For the third approach, the nonspecific adsorption test was conducted in the absence of antibody on the fiber surface. The fiber was modified with AUTES and SBSi and activated by DSS in the same manner as mentioned earlier except the antibody was not immobilized on the fiber surface. The surface was then blocked using ethanolamine. A solution of AuNP@Amp conjugate was then injected in the sensor chip.

Preparation of standard (calibrator) samples in buffer and milk samples

Solutions of ampicillin sodium salt (M.W. = 371.39) were prepared in PBS solution with concentrations ranging from 40,000 ppb (4×10^{-5} g/mL) to 4 ppb (4×10^{-9} g/mL). The milk samples were prepared by spiking different concentrations of ampicillin and then were pretreated using an earlier reported method [23] but with slight modification as in the following way. After spiking 2-mL milk samples, 2 mL of PBS was added to the solution and was blended for 20 min. Ethyl acetate (7 mL) was added to the solution and was shaken vigorously on vortex for 45 min. This solution was then centrifuged for 20 min at 4000 r.p.m. at 4 °C. The supernatant was removed and the centrifugation process was repeated again. The excess ethyl acetate was removed from the supernatant by gentle nitrogen blowing. The dry residue was then dissolved in 2 mL PBS.

Results and discussion

Traditional assay

The assay was first done using the traditional label-free direct assay in FOPPR biosensor [26] as shown in Fig. 1a without using the compound Amp@MUA, since the traditional assay is simple in design and easy to use [26]. The experimental procedure for the traditional assay is described in more detail in the Supplementary Material. In the traditional assay, ampicillin is first tethered covalently to a mixed self-assembled monolayer (SAM) containing MUA and MCH on the surface

of AuNPs which were immobilized on an optical fiber. The ratio of MUA and MCH was used according to a previous study [31] where it was observed that a ratio of 1:4 yield optimum results. The hydrophilic terminal hydroxyl group of MCH in the mixed SAM is employed to minimize nonspecific adsorption [40, 41]. The results of nonspecific adsorption tests were shown in Fig. S1 of the Supplementary Material. When the antibody molecule in sample solution bind with the immobilized ampicillin, it causes a change in the refractive index (RI) of the local medium thus generating a biosensor signal due to the change of plasmon resonance condition [26, 27], as shown in Fig. S2 of the Supplementary Material. The LOD obtained by this method was found to be 1.3×10^{-6} g/mL which is much higher than the MRL for β-lactams antibiotics in food; thus, a more sensitive competitive method based on the principle of fiber optic nanogold-linked immunosorbent assay (FONLISA) [28] had to be developed to improve the sensitivity of the assay for β-lactams antibiotics.

FONLISA

This assay is a surface competitive assay where the unlabeled free ampicillin molecules compete with the ampicillin attached to the AuNPs (AuNP@Amp) to bind with the antibody immobilized on the fiber core surface, as shown in Fig. 1b. In the absence of free ampicillin molecules, there will be absence of competition and the "blank" containing AuNP@Amp conjugates will have the maximum binding with the immobilized antibody molecules, this binding leads to a maximum decrease in transmitted light intensity (I_M) through the sensor fiber relative to that in a buffer (I_0). In the presence of different concentrations of free ampicillin mixed with a fixed concentration of AuNP@Amp conjugates, there is a competition between free ampicillin molecules and AuNP@Amp conjugates for the antibody binding sites. Thus, the higher the concentration of free ampicillin molecules in a tested sample, the lower the amount of AuNP@Amp conjugates that bind to the immobilized antibody on the fiber surface, so lower is the decrease in transmitted light intensity (I_S).

Characterization of AuNPs

The AuNP solution was characterized by a UV-visible spectrophotometer (Jasco, V-570). The peak wavelength was at about 520 nm and the peak absorbance was about 3.0. This AuNP solution was further diluted by 0.12% sodium citrate solution until the absorbance was 2.0 (Fig. S3) and was used as a stock AuNP solution. Histograms of the images derived from transmission electron microscopy (TEM) revealed that the mean diameter of the AuNPs was 12.2 ± 0.7 nm (inset of Fig. S3). The particle concentration of the AuNPs in the stock solutions was about 16.6 nM, estimated by using a molar extinction coefficient of 1.99×10^8 M^{-1} cm^{-1} at the wavelength of 520 nm for this core size of AuNP [42]. Such a particle concentration is overestimated as the molar extinction coefficient of a modified AuNP is larger than that of an unmodified AuNP.

Characterization of MUA–Amp conjugate

The identification of the compound was confirmed by high-resolution electrospray ionization-mass spectrometry (HRMS-ESI).

Figure 4 shows the ESI-mass spectrum of MUA–Amp. The main peak was observed at 572.22 which confirms the formation of the desired product. As can be seen from the data, the mass calculated theoretically for $C_{27}H_{39}N_3NaO_5S_2$ (M^++H) is 572.2229 and from the spectra, it was found to be 572.2220. The other two smaller peaks around 572 are due to the isotopes of the same compound (M^{+2}, M^{+3}). The peak at 561.30 is due to an unknown impurity

The compound was further characterized by FTIR spectroscopy, with spectral peaks listed below and spectra shown in the Supplementary Material (Fig. S4 and S5).

FTIR neat (ampicillin) (Fig. S4): 3366, 3295, 3060, 3032, 2970, 2929, 2866, 1767, 1676, 1607, 1511, 1454, 1400, 1320, 1247, 1206, 1158, 1126, 1070, 1028, 954, 890 cm^{-1}. The stretching vibrations at 1767 cm^{-1}, 1676 cm^{-1}, and 1607 cm^{-1} are due to carbonyl group present in beta-lactam ring, amide, and carboxylic acid salt, respectively. The absorption at 2929 cm^{-1} and 2970 cm^{-1} is due to the presence of two methyl groups in the compound. The stretching frequency at 2866 cm^{-1} represents the methylene groups of the side chain.

FTIR neat (MUA–Amp) (Fig. S5): 3331, 3035, 2928, 2852, 2624, 1773, 1692, 1628, 1576, 1527, 1455, 1387, 1310, 1243, 1185, 1124, 1084, 893, 803 cm^{-1}.

It is observed from the FTIR spectrum that the two weak absorption bands for primary amine from ampicillin that can be observed at 3366 cm^{-1} and 3295 cm^{-1} are replaced by one sharp band at 3331 cm^{-1} which represents the secondary amide N–H stretching, and so, the formation of the bond between ampicillin and MUA can be confirmed [35, 43].

Quantitation of antibody immobilized on the fiber

Assuming that the number of antibody molecules that can be immobilized on the fiber surface depends upon the method on immobilization and not on the type of the antibody, a method based on enzyme-linked immunosorbent assay (ELISA) was developed where mouse IgG was used instead of the anti-penicillin antibody to quantify the amount of antibody molecules immobilized on the fiber surface. Since both the antibodies are IgG molecules, it can be assumed that the results will be similar if the experiment is done with anti-penicillin antibody or with any other IgG antibody.

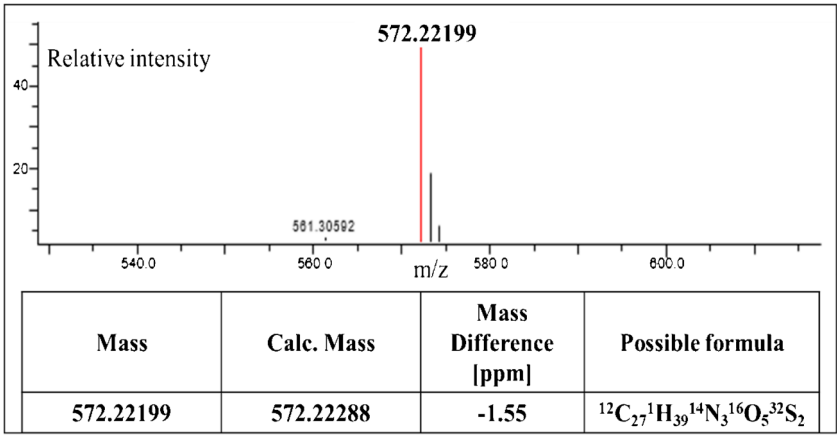

Mass	Calc. Mass	Mass Difference [ppm]	Possible formula
572.22199	572.22288	-1.55	$^{12}C_{27}{}^{1}H_{39}{}^{14}N_{3}{}^{16}O_{5}{}^{32}S_{2}$

Fig. 4 ESI-HRMS calculated for the synthesized MUA–Amp conjugate $C_{27}H_{39}N_3NaO_5S_2$ (M^++H): 572.2229; found 572.2220

The calibration graph for the ELISA experiment is shown in Fig. S6 of the Supplementary Material. The amount of antibody molecules on the fiber surface with a surface area of 25.1 mm^2 was found to be 9.47 ± 0.36 ng. Considering that the molecular weight of the IgG molecule is about 150 kD, the number of antibody molecules per square micrometer was calculated to be 1.51×10^3 molecules/μm^2. This number is about 8.9% of the theoretical value of the maximum number of IgG molecules that can be bound on a surface to form a close-packed monolayer (see Supplementary Material for details in calculations).

Nonspecific adsorption

The prevention of nonspecific adsorption enables more sensitive detection of the target and also rules out the probability of false positives signals. Since AuNPs are used as a detection probe in this biosensor to detect the target, it is important to determine the effect of nonspecific background adsorption of AuNP@Amp on the fiber surface. The success of this method relies on the prevention of such background adsorption. In this regard, MCH was used in AuNP@Amp as a diluent in the mixed SAM using its hydrophilic terminal hydroxyl group to avoid flocculation of AuNP@Amp [44] and to minimize the above effect [40, 41]. The three different methods used here cover all the possibilities that may lead to nonspecific adsorption.

When the AuNPs were coated only with MCH, it was found that no specific binding occurs between AuNP@MCH and the fiber surface. This is evident from the minor change in the intensity as can be seen from Fig. 5a. The average change of normalized transmitted light intensity ($\Delta I/I_0$, where $\Delta I = I_0 - I_S$) was found to be (0.000353 ± 0.000172), based on the average of 3 measurements. Nonspecific adsorption was also tested using AuNP@BSA, a typical sensorgram is shown in Fig. 5b. Based on the average of 3 measurements of the intensity (I) in the AuNP@BSA samples, results show that $\Delta I/I_0$ was 0.000478 ± 0.000089. The signal changes in the above two cases are negligible when compared with $\Delta I/I_0$ for the binding of AuNP@Amp with the anti-penicillin antibody on the fiber surface as shown in Fig. 5d.

A control experiment was also performed by injecting a solution of AuNP@Amp into a sensor chip containing a fiber without an anti-penicillin antibody on the fiber surface. A typical sensorgram is shown in Fig. 5c. Based on the average of three measurements, results show that $\Delta I/I_0$ was 0.000445 ± 0.000108, which is about three hundred times lower than the value obtained when the binding between AuNP@Amp and anti-penicillin antibody occurs as shown in Fig. 5d. This indicates that there is no nonspecific adsorption of AuNP@Amp on the fiber surface and also that the anti-penicillin antibody immobilized on the surface remains functional after the immobilization process.

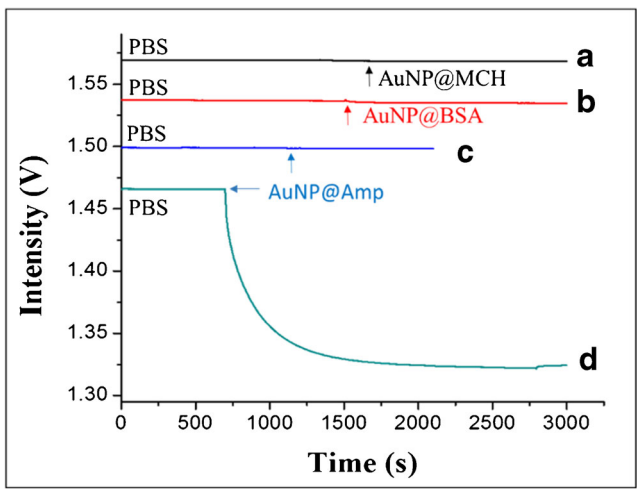

Fig. 5 Real-time sensorgrams showing the responses of the sensor fibers for injection of (a) a solution of AuNP@MCH; (b) a solution of AuNP@BSA; (c) a solution of AuNP@Amp in the absence of antibody on fiber surface; and (d) a solution of AuNP@Amp in the presence of anti-penicillin antibody on the fiber surface. For (a) and (c), the curves have been offset on the *y*-axis to provide a better visual comparison

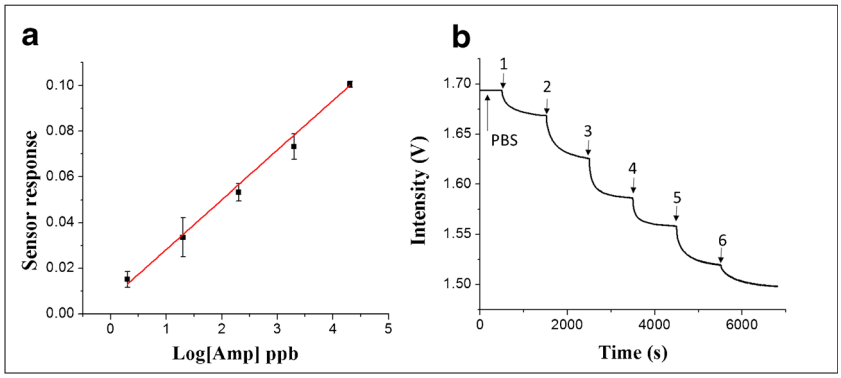

Fig. 6 **a** Calibration curve for the sensor. Sensor response = $(I_S - I_M)/I_0$. Each point is the mean of 3 measurements ± SD. **b** A representative sensorgram. Steps 1 to 6 in the sensorgram represent the free ampicillin concentrations of (1) 2×10^{-5} g/mL, (2) 2×10^{-6} g/mL, (3) 2×10^{-7} g/mL, (4) 2×10^{-8} g/mL, (5) 2×10^{-9} g/mL, and (6) 0 g/mL in the presence of AuNP@Amp conjugates

Quantitative analysis of ampicillin in buffer and milk samples

The experiments for the standard calibration curve were carried out by mixing the solutions of ampicillin with concentrations ranging from 40,000 ppb (4×10^{-5} g/mL) to 4 ppb (4×10^{-9} g/mL) with a solution of AuNP@Amp conjugates in a volume ratio of 1:1. These solutions were then injected serially into the sensor chips containing a sensor fiber using a syringe pump.

The sensorgram and the calibration curve are shown in Fig. 6. Here $\Delta I_M = I_0 - I_M$ represents the change of normalized transmitted light intensity for the average of "blank" readings (0.1163 ± 0.000651, $n = 3$) which is the signal obtained for AuNP@Amp conjugates in the absence of free ampicillin. The linear regression equation was $y = 0.00653 + 0.02175x$ and the correlation coefficient was $r^2 = 0.996$. As the definition of LOD in general does not consider nonspecific adsorption, which could lead to the false-positive signal due to background adsorption of AuNP@Amp on the fiber surface by this approach. Therefore, in this method, two definitions of LOD and LOQ are used. The ideal LOD is defined at a signal-to-noise of 3 where nonspecific background adsorption of AuNP@Amp on the fiber surface is absent and only system noise is considered, while the practical LOD considers the practical effect of such background adsorption and is defined as the mean plus 3 times the standard deviations for the "blank" readings. Thus, the ideal LOD was calculated to be 0.51 ppb (0.51 ng/mL) and the ideal limit of quantification (LOQ) defined by a signal-to-noise of 10 was calculated to be 0.53 ppb (0.53 ng/mL). Because of the very low system noise (relative standard deviation of transmitted light intensity in PBS = 0.0000570), the calculated LOD and LOQ are very close. On the other hand, when the uncertainty due to nonspecific background adsorption of AuNP@Amp on the fiber surface is considered, the practical LOD was calculated to be 0.74 ppb (0.74 ng/mL) and the practical LOQ calculated as 10 times the standard deviations for the "blank" is 1.8 ppb (1.8 ng/mL). A sensorgram showing the signal for ampicillin at a concentration of 1.5 ppb which is near the practical LOQ is shown in Fig. S7 of the Supplementary Material. The method is highly reproducible with a coefficient of variation (CV) less than 9% for the whole concentration range.

At this research stage, the AuNP@Amp had to be freshly prepared each time before the experiment as it was observed that aggregation started to occur in the AuNP solution after 24 h even if refrigerated at 4 °C. The stability of these nanoparticles could be improved by using suitable cryoprotectant and then lypholization of the solution [45]. The antibody-functionalized sensor fibers stored in dried conditions showed more stability and could be used for up to months after modification.

To investigate the accuracy and precision of this assay, recovery experiments were performed by using milk samples spiked with different concentrations of ampicillin. The results are summarized in Table 1. The percentages of recovery are between 94.69 and 102.50% while the CV is less than 5.5%, indicating good detection accuracy and reproducibility of the sensor.

Selectivity of the sensor

The selectivity of the sensor was tested by comparing the sensor responses toward different antibiotics. Since the antibody used is sensitive to many β-lactam antibiotics, the antibiotics ampicillin, penicillin, and amoxicillin were

Table 1 Determination of ampicillin in different matrices. Each value is the mean of 3 measurements

Matrix	Amount added (ppb)	Amount determined (ppb)	Recovery (%)	% CV
Pretreated milk ($n = 3$)	10,000	10,249.51	102.55 ± 3	3.61
	500	484.79	96.96 ± 5.2	5.33
	15	14.60	94.69 ± 4.7	4.97

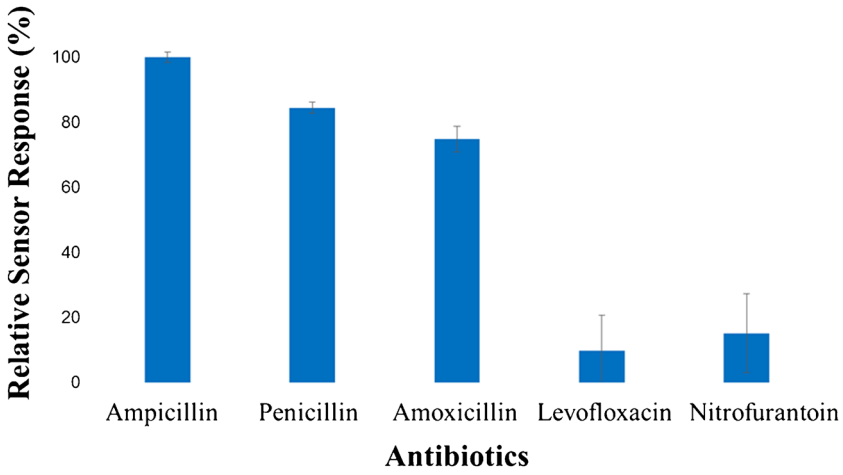

Fig. 7 Selectivity of the sensor for β-lactam vs non-β-lactam antibiotics. Each value is the mean of three readings. The relative sensor response in percent values are ampicillin 100, penicillin G 84.59, amoxicillin 74.87, levofloxacin 9.63, and nitrofurantoin 15.15%, where ampicillin is taken to be 100%

tested, and the non-β-lactam antibiotics levofloxacin and nitrofurantoin were also investigated at the concentration of 2×10^{-5} g/mL. Although the chemical structures of β-lactam antibiotics are similar, the antibody used in this study displays the best reactivity to ampicillin, the response of which was taken as 100%, but there is a considerable level of reactivity toward penicillin G (84.59%) and amoxicillin (74.87%), as shown in Fig. 7. On the other hand, the level of reactivity toward levofloxacin (9.63%) and nitrofurantoin (15.15%) is small, indicating good detection selectivity of the sensor.

Comparison with other reported ampicillin biosensors

The comparison of detection performances with different biosensors is shown in Table 2. As can be seen, this biosensor exhibits low practical LOD and a wide linear range. In addition, the biosensor analysis time without consideration of the sample pretreatment steps is less than 15 min. Furthermore, the instrument used in this work is inexpensive and has a great potential to be miniaturized into a portable biosensor, thus making the biosensor ideal as a field-based screening tool for the detection of ampicillin and other β-lactams in milk. Since the sensor chips used in this biosensor are low cost, the reusability of the sensor chips was not determined.

Conclusion

This work shows a simple, fast, and sensitive biosensor and method for the detection of ampicillin well below the MRL advised by the European Union and WHO. The importance of having a sensitive biosensor for the detection of antibiotics lies in the following three considerations. First, to reduce the false-negative rate, LOD should be lower than or at least equal to MRL. Second, a high precision around MRL is a decisive factor in quality control. In general, the CV value increases at decreasing analyte concentration [48, 49]. As such, LOQ should be lower than or at least equal to MRL. Third, analysis of real samples often requires dilution of the real samples such as milk samples to reduce the matrix effect, thus requiring LOD lower than MRL to incorporate the dilution effect. Furthermore, this biosensor also provides a wide linear range (4 orders) for the quantitative determination of ampicillin in real samples such as milk, making detection of real samples having a wide concentration range more convenient. This sensor can be slightly modified by changing the antibiotic attached to the probe and then can be used for the detection of other β-lactam antibiotics at very low concentrations. Thus, this sensor can be used as a fast pre-screening method to detect the presence or absence of antibiotics in samples. Alternatively, this sensor can also be modified by using one of the penicillin-binding proteins (PBPs) instead of the

Table 2 Comparison of detection performances of different ampicillin biosensors

Detection Method	LOD	Reference
Microwave electrodynamic resonator using *E. coli*	4000 ng/mL	[46]
Surface plasmon resonance biosensor	2 ng/mL	[22]
Amperometry	4 ng/mL	[47]
Resonant waveguide grating biosensor	3.1 ng/mL	[19]
Gold nanoparticle-based dual fluorescence–colorimetric method	2 ng/mL	[23]
FOPPR biosensor	0.74 ng/mL	This work

antibody as these proteins bind covalently with more number of antibiotics as compared with the antibody [22].

Acknowledgments We thank Prof. Bor-Cherng Hong for helpful advice on the synthesis and characterization of Amp–MUA conjugate.

Authors' contributions Conceptualization, Lai-Kwan Chau; methodology, Lai-Kwan Chau and Yuh-Ling Chen; resources, Chun-Jen Huang; investigation, Pallavi Chaudhari and Yen-Ta Tseng; formal analysis, Pallavi Chaudhari, Lai-Kwan Chau, and Yen-Ta Tseng; writing - original draft, Pallavi Chaudhari; writing - review and editing, Lai-Kwan Chau; funding acquisition, Lai-Kwan Chau.

Funding information This work was supported by the Ministry of Science and Technology of Taiwan (Grant no. MOST 105-2113-M-194-009-MY3) and Center for Nano Bio-Detection from the Featured Research Areas College Development Plan of National Chung Cheng University.

Availability of data and material All data generated or analyzed during this study are included in this published article and its supplementary material file.

Compliance with ethical standards

Conflict of interest The authors declare that they have no conflict of interest.

Code availability Not applicable

References

1. Rosegrant MW, Fernandez M, Sinha A, et al (2009) Looking into the future for agriculture and AKST. Retrived from https://hdl.handle.net/10568/37336. Accessed 3 Mar 2019
2. Preston RL (1988) The role of animal drugs in food animal production. Symposium on Animal Drug Use - Dollars and Sense, Washington. pp. 127–133
3. Silbergeld EK, Graham J, Price LB (2008) Industrial food animal production, antimicrobial resistance, and human health. Annu Rev Public Health 29:151–169. https://doi.org/10.1146/annurev.publhealth.29.020907.090904
4. Council NR (1980) The effects on human health of subtherapeutic use of antimicrobials in animal feeds. National Academies Press, Washington, D.C.
5. Landers TF, Cohen B, Wittum TE, Larson EL (2012) A review of antibiotic use in food animals: perspective, policy, and potential. Public Health Rep 127:4–22. https://doi.org/10.1177/003335491212700103
6. Economou V, Gousia P (2015) Agriculture and food animals as a source of antimicrobial-resistant bacteria. Infect Drug Resist 8:49–61. https://doi.org/10.2147/IDR.S55778
7. Angulo FJ, Baker NL, Olsen SJ et al (2004) Antimicrobial use in agriculture: controlling the transfer of antimicrobial resistance to humans. In: Seminars in pediatric infectious diseases. Elsevier, In, pp 78–85
8. Berends BR, van den Bogaard AE, Van Knapen F, Snijders JM (2001) Human health hazards associated with the administration of antimicrobials to slaughter animals. Part II. An assessment of the risks of resistant bacteria in pigs and pork. Vet Q 23:10–21. https://doi.org/10.1080/01652176.2001.9695069
9. Xie K, Jia L, Xu D, Guo H, Xie X, Huang Y, Chen X, Bao W, Dai G, Wang J (2012) Simultaneous determination of amoxicillin and ampicillin in eggs by reversed-phase high-performance liquid chromatography with fluorescence detection using pre-column derivatization. J Chromatogr Sci 50:620–624. https://doi.org/10.1093/chromsci/bms052
10. Cháfer-Pericás C, Maquieira A, Puchades R (2010) Fast screening methods to detect antibiotic residues in food samples. Trends Anal Chem 29:1038–1049
11. Olstege DMH, Uschner BP, Hitehead GW (2002) Screening and mass spectral confirmation of β-lactam antibiotic residues in milk using LC-MS/MS. J Agri Food Chem 50:406–411. https://doi.org/10.1021/jf010994s
12. Bogialli S, Capitolino V, Curini R, di Corcia A, Nazzari M, Sergi M (2004) Simple and rapid liquid chromatography−tandem mass spectrometry confirmatory assay for determining amoxicillin and ampicillin in bovine tissues and milk. J Agric Food Chem 52:3286–3291. https://doi.org/10.1021/jf0499572
13. Stolker AAM, Rutgers P, Oosterink E, Lasaroms JJP, Peters RJB, van Rhijn JA, Nielen MWF (2008) Comprehensive screening and quantification of veterinary drugs in milk using UPLC–ToF-MS. Anal Bioanal Chem 391:2309–2322. https://doi.org/10.1007/S00216-008-2168-8
14. Kantiani L, Farre M (2009) Analytical methodologies for the detection of β-lactam antibiotics in milk and feed samples. Trends Anal Chem 28(6):729–744. https://doi.org/10.1016/j.trac.2009.04.005
15. Babington R, Matas S, Marco M (2012) Current bioanalytical methods for detection of penicillins. Anal Bioanal Chem 403:1549–1566. https://doi.org/10.1007/s00216-012-5960-4
16. FitzGerald SP, O'Loan N, McConnell RI et al (2007) Stable competitive enzyme-linked immunosorbent assay kit for rapid measurement of 11 active beta-lactams in milk, tissue, urine, and serum. J AOAC Int 90:334–342
17. Benito-Peña E, Moreno-Bondi MC, Orellana (2005) Development of a novel and automated fluorescent immunoassay for the analysis of β-lactam antibiotics. J Agri Food Chem 53(17):6635–6642. https://doi.org/10.1021/jf0511502
18. Gustavsson E, Bjurling P, Sternesjö Å (2002) Biosensor analysis of penicillin G in milk based on the inhibition of carboxypeptidase activity. Anal Chim Acta 468:153–159
19. Adrian J, Pasche S, Voirin G, Adrian J, Pinacho DG, Font H, Sánchez-Baeza F, Marco MP, Diserens JM, Granier B (2009) Wavelength-interrogated optical biosensor for multi-analyte screening of sulfonamide, fluoroquinolone, β-lactam and tetracycline antibiotics in milk. Trends Anal Chem 28:769–777. https://doi.org/10.1016/J.TRAC.2009.04.011
20. Gaudin V, Fontaine J, Maris P (2001) Screening of penicillin residues in milk by a surface plasmon resonance-based biosensor assay: comparison of chemical and enzymatic sample pre-treatment. Anal Chim Acta 436:191–198. https://doi.org/10.1016/S0003-2670(01)00948-5
21. Byzova NA, Zvereva EA, Zherdev AV, Dzantiev BB (2011) Immunochromatographic technique for express determination of ampicillin in milk and dairy products. Appl Biochem Microbiol 47:627–634. https://doi.org/10.1134/S0003683811060032
22. Cacciatore G, Petz M, Rachid S, Hakenbeck R, Bergwerff AA (2004) Development of an optical biosensor assay for detection of β-lactam antibiotics in milk using the penicillin-binding protein 2x*. Anal Chim Acta 520:105–115. https://doi.org/10.1016/j.aca.2004.06.060
23. Song K-M, Jeong E, Jeon W, Cho M, Ban C (2012) Aptasensor for ampicillin using gold nanoparticle based dual fluorescence–colorimetric methods. Anal Bioanal Chem 402:2153–2161. https://doi.org/10.1007/s00216-011-5662-3
24. Karaseva N, Ermolaeva T, Mizaikoff B (2016) Piezoelectric sensors using molecularly imprinted nanospheres for the detection of

antibiotics. Sens Actuat B 225:199–208. https://doi.org/10.1016/j.snb.2015.11.045
25. Puchades R, Cha C (2010) Fast screening methods to detect antibiotic residues in food samples. Trends Anal Chem 29(9):1038–1049. https://doi.org/10.1016/j.trac.2010.06.004
26. Cheng S-F, Chau L-K (2003) Colloidal gold-modified optical fiber for chemical and biochemical sensing. Anal Chem 75:16–21. https://doi.org/10.1021/ac020310v
27. Chau L-K, Lin Y-F, Cheng S-F, Lin T-J (2006) Fiber-optic chemical and biochemical probes based on localized surface plasmon resonance. Sens Actuat B 113:100–105. https://doi.org/10.1016/j.snb.2005.02.034
28. Chiang C-Y, Huang T-T, Wang C-H, Huang CJ, Tsai TH, Yu SN, Chen YT, Hong SW, Hsu CW, Chang TC, Chau LK (2020) Fiber optic nanogold-linked immunosorbent assay for rapid detection of procalcitonin at femtomolar concentration level. Biosens Bioelectron 151:111871
29. Otte MA, Estévez MC, Regatos D, Lechuga LM, Sepúlveda B (2011) Guiding light in monolayers of sparse and random plasmonic meta-atoms. ACS Nano 5(11):9179–9186. https://doi.org/10.1021/nn203432z
30. Wu W-T, Chen C-H, Chiang C-Y, Chau L-K (2018) Effect of surface coverage of gold nanoparticles on the refractive index sensitivity in fiber-optic nanoplasmonic sensing. Sensors 18(6):1759. https://doi.org/10.3390/s18061759
31. Chiang C-Y, Hsieh M-L, Huang K-W, Chau LK, Chang CM, Lyu SR (2010) Fiber-optic particle plasmon resonance sensor for detection of interleukin-1β in synovial fluids. Biosens Bioelectron 26:1036–1042. https://doi.org/10.1016/J.BIOS.2010.08.047
32. Yeh S-B, Chen C-S, Chen W-Y, Huang C-J (2014) Modification of silicone elastomer with zwitterionic silane for durable antifouling properties. Langmuir 30(38):11386–11393. https://doi.org/10.1021/la502486e
33. Huang Y-C, Chiang C-Y, Li C-H, Chang TC, Chiang CS, Chau LK, Huang KW, Wu CW, Wang SC, Lyu SR (2013) Quantification of tumor necrosis factor-α and matrix metalloproteinases-3 in synovial fluid by a fiber-optic particle plasmon resonance sensor. Analyst 138:4599–4606. https://doi.org/10.1039/C3AN00276D
34. Chen W-H, Tseng Y-T, Hsieh S, Liu WC, Hsieh CW, Wu CW, Huang CH, Lin HY, Chen CW, Lin PY, Chau LK (2014) Silanization of solid surfaces via mercaptopropylsilatrane: a new approach of constructing gold colloid monolayers. RSC Adv 4:46527–46535. https://doi.org/10.1039/C4RA05583G
35. Franchini MC, Bonini BF, Camaggi CM et al (2010) Design and synthesis of novel 3,4-disubstituted pyrazoles for nanomedicine applications against malignant gliomas. Eur J Med Chem 45:2024–2033. https://doi.org/10.1016/j.ejmech.2010.01.014
36. Aslan K, Pérez-Luna VH (2002) Surface modification of colloidal gold by chemisorption of alkanethiols in the presence of a nonionic surfactant. Langmuir 18:6059–6065. https://doi.org/10.1021/la025795x
37. Finklea HO, Liu L, Ravenscroft MS, Punturi S (1996) Multiple electron tunneling paths across self-assembled monolayers of alkanethiols with attached ruthenium(II/III) redox centers. J Phys Chem 100(48):18852–18858. https://doi.org/10.1021/JP962831Q
38. Brevnov DA, Finklea HO (2000) Alternating current voltammetry studies of the effect of melittin on heterogeneous electron transfer across a hybrid bilayer membrane supported on a gold electrode. Langmuir 16(14):5973–5979. https://doi.org/10.1021/la9915217
39. Hsu W-T, Hsieh W-H, Cheng S-F, Jen CP, Wu CC, Li CH, Lee CY, Li WY, Chau LK, Chiang CY, Lyu SR (2011) Integration of fiber optic-particle plasmon resonance biosensor with microfluidic chip. Anal Chim Acta 697:75–82
40. Prime KL, Whitesides GM (1991) Self-assembled organic monolayers: model systems for studying adsorption of proteins at surfaces. Science (80):1164–1167
41. Silin V, Weetall H, Vanderah DJ (1997) SPR studies of the nonspecific adsorption kinetics of human IgG and BSA on gold surfaces modified by self-assembled monolayers (SAMs). J Colloid Interface Sci 185:94–103
42. Liu X, Atwater M, Wang J, Huo Q (2007) Extinction coefficient of gold nanoparticles with different sizes and different capping ligands. Colloids Surf B 58:3–7. https://doi.org/10.1016/j.colsurfb.2006.08.005
43. Elmes RBP, Orange KN, Cloonan SM, Williams DC, Gunnlaugsson T (2011) Luminescent ruthenium(II) polypyridyl functionalized gold nanoparticles: their DNA binding abilities and application as cellular imaging agents. J Am Chem Soc 133:15862–15865. https://doi.org/10.1021/ja2061159
44. Weisbecker CS, Merritt MV, Whitesides GM (1996) Molecular self-assembly of aliphatic thiols on gold colloids. Langmuir 12:3763–3772
45. Alkilany AM, Abulateefeh SR, Mills KK, Bani Yaseen AI, Hamaly MA, Alkhatib HS, Aiedeh KM, Stone JW (2014) Colloidal stability of citrate and mercaptoacetic acid capped gold nanoparticles upon lyophilization: effect of capping ligand attachment and type of cryoprotectants. Langmuir 30:13799–13808
46. Guliy OI, Zaitsev BD, Smirnov AV, Karavaeva OA, Borodina IA (2019) Sensor for ampicillin based on a microwave electrodynamic resonator. Biosens Bioelectron 130:95–102 S0956566319300533
47. Gamella M, Campuzano S, Conzuelo F, Esteban-Torres M, de las Rivas B, Reviejo AJ, Muñoz R, Pingarrón JM (2013) An amperometric affinity penicillin-binding protein magnetosensor for the detection of β-lactam antibiotics in milk. Analyst 138:2013–2022
48. Horwitz W (1982) Evaluation of analytical methods used for regulation of foods and drugs. Anal Chem 54:67–76
49. Sadler WA (2008) Imprecision profiling. Clin Biochem Rev 29(Suppl 1):S33–S36